RNA Quantification Hot Paper

International Edition: DOI: 10.1002/anie.201814377
German Edition: DOI: 10.1002/ange.201814377

Absolute Quantification of Noncoding RNA by Microscale Thermophoresis

*Dominik Jacob[+], Kathrin Thüring[+], Aurellia Galliot, Virginie Marchand, Adeline Galvanin, Akif Ciftci, Karin Scharmann, Michael Stock, Jean-Yves Roignant, Sebastian A. Leidel, Yuri Motorin, Raffael Schaffrath, Roland Klassen, and Mark Helm**

Abstract: *Accurate quantification of the copy numbers of noncoding RNA has recently emerged as an urgent problem, with impact on fields such as RNA modification research, tissue differentiation, and others. Herein, we present a hybridization-based approach that uses microscale thermophoresis (MST) as a very fast and highly precise readout to quantify, for example, single tRNA species with a turnaround time of about one hour. We developed MST to quantify the effect of tRNA toxins and of heat stress and RNA modification on single tRNA species. A comparative analysis also revealed significant differences to RNA-Seq-based quantification approaches, strongly suggesting a bias due to tRNA modifications in the latter. Further applications include the quantification of rRNA as well as of polyA levels in cellular RNA.*

The three classes of RNA directly required for protein biosynthesis comprise the overwhelming majority of cellular RNA. rRNAs and tRNAs make up approximately 80–90% and 5–10%, respectively, with mRNA and other less abundant species accounting for the remainder. Most recent developments in RNA quantification concern library preparations for RNA-Seq. These address specific mRNA sequences, but also the composition and length of the polyA tail.[1] Concerning noncoding RNAs, several recent reports particularly focused on tRNA quantification. While these approaches require low amounts of total tRNA, the multistep enzymatic transformations innate to RNA-Seq make calibration inherently difficult. Furthermore, modified nucleotides induce biases in addition to those already present in RNA-Seq.[2] Other methods used for the quantification of single RNA species, such as qPCR, northern blot, and microchips, are all geared towards providing changes in RNA abundance relative to a standard. In contrast, the only tangible solution for absolute quantification with any of the above methods requires a calibration curve, that is, a time-consuming comparison to a standard of known quantity.

To avoid the biases of RNA-Seq, we herein present a hybridization-based approach that makes use of the high affinity of complementary DNA (cDNA) for RNA. Considering that the K_D values are in the pM range for a 16mer-cDNA,[3] a full-length cDNA can be safely assumed to quantitatively hybridize to its complementary tRNA at least in the nM range. In titration experiments, constant amounts of fluorescently labeled cDNA probes (FCPs) were hybridized with increasing amounts of target tRNA, here an in vitro transcript (IVT) of $tRNA^{Met}_{(CAU)}$ from *E. coli*. To determine the amount of tRNA–cDNA duplex, we tested both an electrophoretic mobility shift assay (EMSA) on non-denaturing PAGE and microscale thermophoresis (MST). MST uses fluorescence detection to monitor the directed diffusion of biomolecules along a temperature gradient for the quantitative analysis of bimolecular binding events.[3,4] To measure hybridization precisely, we took a cue from data treatment common in the determination of K_D values of macromolecular complexes. A typical plot of complex versus ligand concentration on a logarithmic scale yields a classical sigmoidal curve.[5] The inflection point, corresponding to 50% of bound ligand, is a half-maximum value,

[*] D. Jacob,[+] K. Thüring,[+] A. Galliot, Prof. Dr. M. Helm
Institute of Pharmacy and Biochemistry
Johannes Gutenberg University Mainz
Staudingerweg 5, 55128 Mainz (Germany)
E-mail: mhelm@uni-mainz.de

Dr. V. Marchand
Lorraine University, UMS2008 IBSLor CNRS-UL-INSERM, Biopôle UL
9, Avenue de la Forêt de Haye, 54505 Vandoeuvre-les-Nancy (France)

A. Galvanin, Prof. Dr. Y. Motorin
Lorraine University, UMR7365 IMoPA CNRS-UL, Biopôle UL
9, Avenue de la Forêt de Haye, 54505 Vandoeuvre-les-Nancy (France)

A. Ciftci
Institute for Biochemistry and Molecular Biology
Faculty of Medicine, University of Freiburg
Stefan-Meier-Str. 17, 79104 Freiburg (Germany)

K. Scharmann, Dr. S. A. Leidel
Max Planck Research Group for RNA Biology
Max Planck Institute for Molecular Biomedicine
Von-Esmarch-Str. 54, 48149 Münster (Germany)

M. Stock, J.-Y. Roignant
Institute of Molecular Biology
Ackermannweg 4, 55128 Mainz (Germany)

Prof. Dr. R. Schaffrath, Dr. R. Klassen
Institut für Biologie, Fachgebiet Mikrobiologie
Universität Kassel
Heinrich-Plett-Str. 40, 34132 Kassel (Germany)

[+] These authors contributed equally to this work.

Supporting information and the ORCID identification number(s) for the author(s) of this article can be found under: https://doi.org/10.1002/anie.201814377.

that is, in typical applications, essentially equivalent to the K_D value.

In contrast, the low K_D value of cDNA in tRNA binding means that the inflection point (EC_{50}) corresponds to the concentration of RNA necessary to hybridize 50% of the FCP. Therefore, at known FCP concentrations, the EC_{50} value provides information on the absolute amount of target RNA present in the sample. Moreover, with the EC_{50} value being situated in a highly dynamic range, various algorithms[6] allow rapid calculation from sigmoidal binding plots, such as those shown in Figure 1, with high accuracy.

Dual analysis (Figure 1a) of the titration of FCP with IVT-$tRNA^{Met}_{(CAU)}$ gave highly consistent results between EMSA (Figure 1b) and MST (Figure 1c). Quantification of free FCP and the tRNA/FCP duplex was straightforward from their respective bands on native PAGE, and followed standard procedures for MST. Based on the fluorescence time trace shown in Figure 1c, values were determined immediately after establishing the temperature gradient by switching on the IR laser ("cold" values in blue) and after relaxation of the system ("hot" values in red). In the particular case of $tRNA^{Met}_{(CAU)}$, the increase in fluorescence between cold and hot indicates a movement of the free FCP into the heated focus, while the tRNA/FCP duplex shows inverse migration (i.e., out of the heated focus). Of note, for most tested tRNA/FCP duplexes, this behavior was inverted, which resulted in reverse directionality for the corresponding sigmoidal curves. Sequence analysis of all used FCPs did not provide any correlation between FCP sequence or length and the direction of thermophoresis of either free FCP or the FCP–RNA hybrid. Most free FCPs showed moderate movement whereas the hybrid displayed more pronounced negative (or, less often, positive) thermophoresis. Importantly, the requirement for hybridization became evident from a lack of response of the MST plot upon omission of an annealing step (see the Supporting Information, Figure S1a).

When expressed as the tRNA/FCP molar ratio, the expected EC_{50} value is 0.5 (i.e., 50%). The values obtained by EMSA and MST were 0.40 and 0.43, respectively (Figure 1d), and thus within 8% of each other and within the typical accuracy error for the quantification of nucleic acids by UV absorption, for example, as a result of hypochromicity (ca. 10–20%).[7] Even more accurate was the MST-EC_{50} value of 0.56 for native, fully modified $tRNA^{Met}_{(CAU)}$ (Figure S1b).

Attempts to shorten the FCP from full-length cDNA were only partially successful. Assays with 20, 30, and 40mer FCPs targeted against various regions of the cloverleaf (Table S4) revealed only slightly less efficient detection with three 40mers, but pronounced loss of signal for shorter FCPs. More importantly, a drastic influence of the target site within the tRNA sequence (3′, 5′, or middle), as well as of modified nucleotides within the native tRNA, was observed (Figure S1c–e) for short FCPs, but not for the full-length FCPs. The latter findings are in agreement with literature on the interference of RNA modifications with proper hybridization in microarray and northern blot experiments using 15–25mer cDNA.[9] In summary, the results of this model characterization confirmed that RNA and full-length FCP hybridized

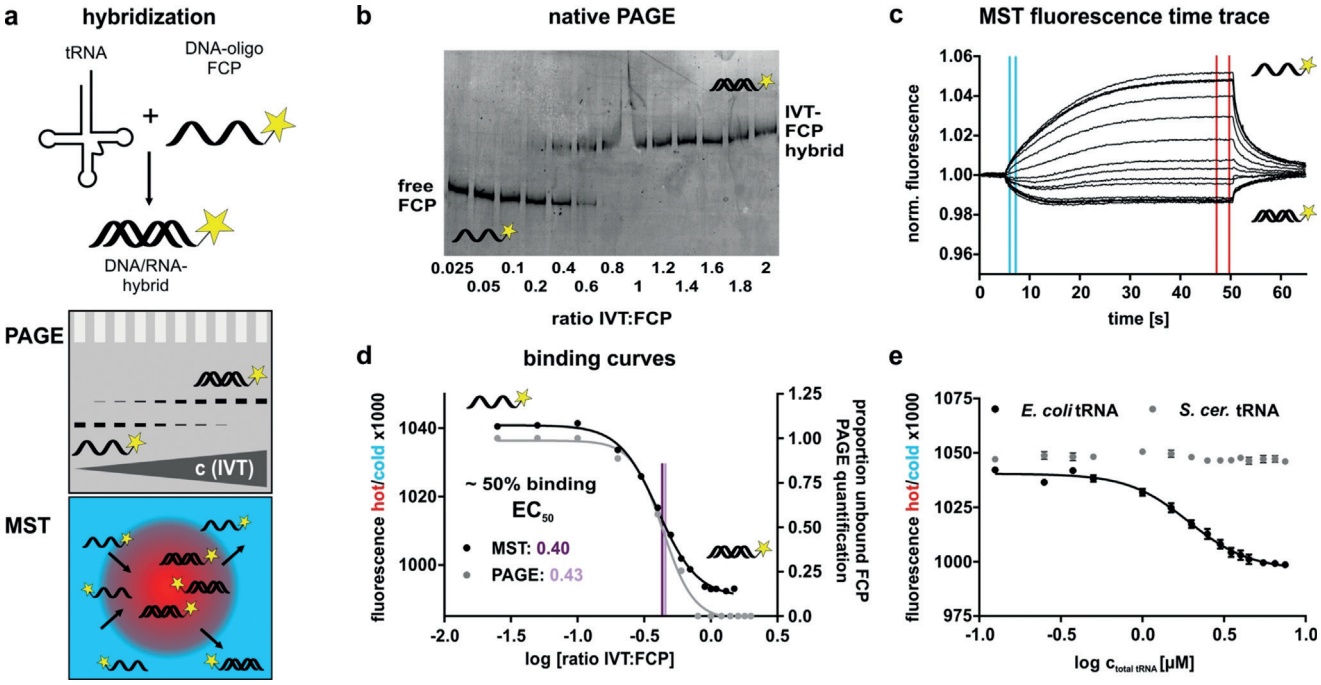

Figure 1. Concept of the absolute quantification by hybridization yield readout. a) Workflow of hybridization yield determination by EMSA and MST. b) EMSA analysis of a dilution series of target IVT, hybridized to a constant amount of FCP. c) Fluorescence time trace recorded for the hybridization of target IVT to its corresponding FCP. Normalized fluorescence values taken from zones delineated in red ("hot") versus blue ("cold") were used to calculate the fluorescence ratio plotted in (d). Similarly, hybridization ratios determined in (b) were plotted for comparison of EMSA versus MST, yielding EC_{50} values within 8% of each other (shown in lilac). e) Response curve of FCP titration with total tRNA from *E. coli* (black) versus *S. cerevisiae* (gray) illustrating FCP specificity for *E. coli* $tRNA^{Met}_{(CAU)}$. Data are given as mean ± SD, $n = 3$ technical replicates.

quantitatively under MST conditions, and suggested MST as a potential method for fast and accurate quantification of tRNAs in biological mixtures. For verification, the FCP was titrated in a dilution series of total tRNA from both yeast and *E. coli*. While the lack of a response in yeast total tRNA illustrated specificity (Figure 1e, gray), a well-defined EC_{50} value was obtained from *E. coli* total tRNA, yielding 1.04 pmol $tRNA^{Met}_{(CAU)}$ in 1 µg total tRNA, corresponding to 2.6% (w/w). Similarly, five other *E. coli* tRNA species in the total tRNA were quantified by MST and validated by EMSA (Figure S1f), with an average deviation of 9% between both methods. We conclude that both methods are equally suitable for absolute quantification. Importantly, MST quantification takes about one hour, making it more than one order of magnitude faster than EMSA and other quantification techniques.

To develop MST into a generally applicable technique for the assessment of various tRNA species, we focused on the tRNA levels in *S. cerevisiae*. Bearing in mind the effects of RNA modifications (Figure S1d,e), 27 FCPs were specifically designed[8] to be as long as possible to assure a K_D value at least in the nM range. Such FCPs will capture all species of near-identical sequences, including, for example, SNPs. In tests with yeast total tRNA, 22 FCPs were found to be suitable for MST analysis under the standard conditions, and screening of pH and salt concentrations eventually also allowed quantification of $tRNA^{Arg}_{(ACG)}$ (Figure S2). Given the still cryptic rules that govern thermophoresis behavior,[10] an explanation as to why the remaining four FCPs did not yield well-defined binding curves in MST is currently lacking.

The impressive precision of the method is illustrated in Figure 2a, where the three tRNA species with the smallest and largest standard deviations (SDs) are depicted. In three technical replicates, the SD ranged from 0.006% to 0.2%. Biological replicates showed equally small variations (Figure 2b). Repeated measurements of $tRNA^{Leu}_{(UAA)}$ in aliquots of the same sample after two months deviated by only about 6%, demonstrating good long-term reproducibility (Figure S3a). Almost identical quantification results were found for $tRNA^{Lys}_{(UUU)}$ from genetic backgrounds of two yeast strains (S288C and BY4741; Figure S3b). In summary, the technique produced values with variations that are clearly smaller than typical nucleic acid quantification errors.[7]

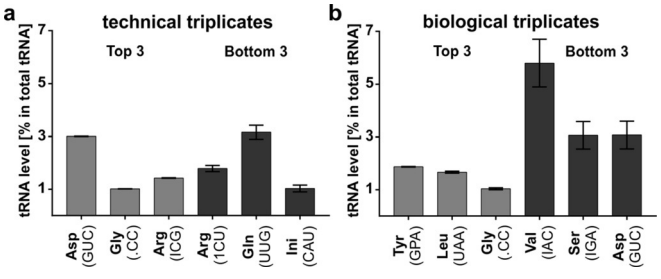

Figure 2. Features of the MST-based tRNA quantification. Three tRNAs with the lowest (gray) or highest (black) SD (% in total tRNA) in technical (a) or biological replicates (b) are shown. Data are mean ± SD, $n = 3$. The SDs range from 0.002 to 0.124 for technical and from 0.007 to 0.17 for biological triplicates.

As a first in a series of applications to biological questions involving altered steady-state levels of tRNAs, the specificity of the *Pichia acacia* killer toxin (PaT), a tRNase with reported preference for $tRNA^{Gln}_{(UUG)}$, was confirmed.[11] Yeast cells expressing PaT showed a dramatic reduction in $tRNA^{Gln}_{(UUG)}$, but the levels of control $tRNA^{His}_{(GUG)}$ were unaffected (Figures 3a,b and S4a). MST further faithfully recapitulated

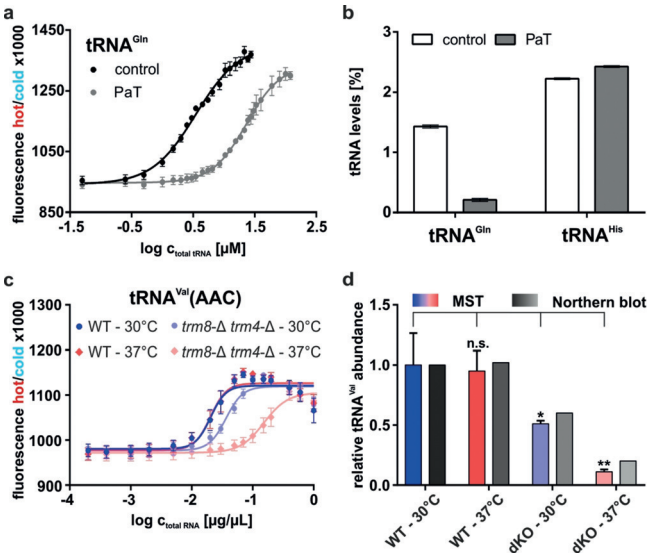

Figure 3. a) MST binding curve for $tRNA^{Gln}_{(UUG)}$ in control (black) and PaT killer toxin treated (gray) *S. cerevisiae* samples. b) Quantification results (% tRNA in total tRNA) for $tRNA^{Gln}_{(UUG)}$ and control $tRNA^{His}_{(GUG)}$. Data equal mean ± SD, $n = 3$ technical replicates. c) MST of $tRNA^{Val}_{(AAC)}$ from WT or *trm8*-Δ-*trm4*-Δ double-mutant *S. cerevisiae* strains grown at 30°C or from cells shifted to 37°C for 3 h. d) Relative tRNA abundances. Data equal mean ± SD, $n = 3$ biological replicates. Corresponding northern blot data from Ref. [12] are in given in black/gray.

a reduction in $tRNA^{Val}_{(AAC)}$ levels due to hypomodification in yeast strains lacking the tRNA modification enzymes Trm8 and Trm4 (Figure 3c,d).[12] The absence of the corresponding post-transcriptional modifications from $tRNA^{Val}_{(AAC)}$ leads to instability and makes it a substrate for the rapid tRNA decay pathway (RTD), an effect that was found to be exacerbated at elevated growth temperatures. By comparison, a control $tRNA^{Arg}_{(ACG)}$, which is not a substrate of either enzyme, remained unaffected (Figure S4b).[12,13] As shown in Figure 3d, we found remarkably accurate agreement between our own MST data and the original data obtained by northern blot analysis,[12] promoting MST as a viable alternative also for relative quantification.

Given the considerably higher speed of MST, we applied the technique to the detection of potential RTD in a larger panel of yeast double mutants lacking enzymes that introduce modifications in the tRNA anticodon stem loop (ASL). These included elongator modifications at U34 (*elp3*), Ψ38, and Ψ39 (*deg1*), thiolation of U34 (*urm1*), and ct^6A37 (*tcd1*).[14] All double mutants displayed synthetic growth defects at elevated temperature, but the effects of the modification defects on tRNA levels remained unknown. MST measurements

allowed the rapid compilation of heat maps from strains grown under two temperature conditions. The analysis, as detailed in Figure S5, suggested that in contrast to the role of structural modifications in the tRNA core,[12,15] the absence of modifications in the ASL did not systematically lead to lower steady-state tRNA levels, excluding the latter as a molecular reason for the growth defects of the mutants.[14] This is in line with the nonstructural role of these modifications, which is thought to be a functional modulation of the decoding properties in the ASL.[16] Hence factors other than RTD seem to be governing the steady-state level of tRNA.

For comparison of MST with RNA-seq-based quantification, we employed a routine that had previously been established for the mapping of tRNA modifications,[17] and was now adapted to the quantification of yeast tRNA. Simultaneously, we used MST to quantify 23 tRNA species in yeast grown at 30 °C and 39 °C, respectively. The latter temperature was established as a condition that ablates thiolation at U34.[18] The results in Figure 4 represent three biological replicates, each measured in three technical replicates. Already the visual inspection of the RNA-Seq-based quantification suggests a few strikingly abundant species along with some of very low abundance, featuring about 100-fold differences. Indeed, such artificially high read numbers are a recognized problem, dubbed "jackpot" tRNA,[2d] which is compounded by the fact that different RNA-Seq protocols differentially amplify different tRNA species.[2a,d,17] A further problem, the opposing underrepresentation of certain species, which presumably is a consequence of RNA post-transcriptional modifications, has not yet been completely resolved, despite some progress.[2a,c,19] In contrast, MST-based quantification yields tRNA steady-state levels that are much more evenly balanced and thus more plausible. The MST results show a clearly better correlation with gene copy number ($R^2 = 0.47$) than the RNA-Seq data ($R^2 = 0.36$, Figure S6).

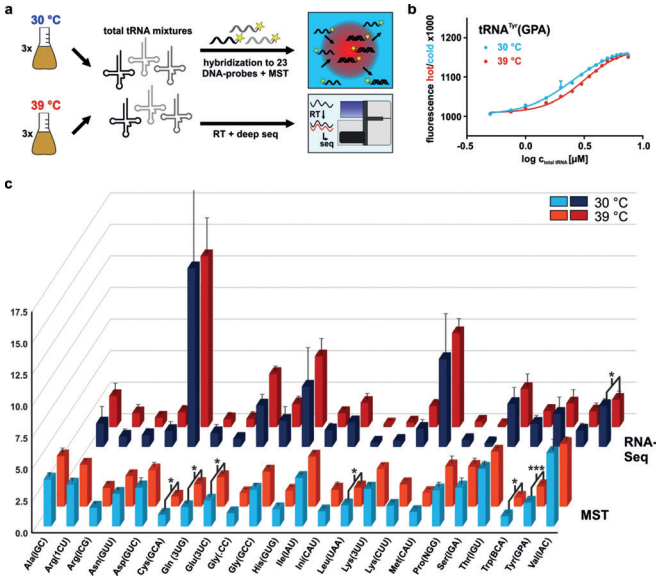

Figure 4. Comparison of MST and RNA-Seq performance in tRNA quantification. a) The *S. cerevisiae* total tRNA was isolated from cultures grown at 30 °C or 39 °C and simultaneously analyzed by MST and RNA-Seq. b) MST curve of $tRNA^{Tyr}_{(GUA)}$ at 30 °C (blue) and 39 °C (red). c) Comparison of quantification results obtained from MST and RNA-Seq for 23 tRNAs at 30 °C and 39 °C. Data equal mean ± SD, $n = 3$ biological replicates.

While it is relevant that the 23 yeast FCPs have not been individually validated for absolute quantification as previously exemplified for *E. coli* $tRNA^{Met}_{(CAU)}$ (Figures 1 and S1), any errors in relative quantification would be based on the same source as for any other hybridization-based technique. A more exhaustive comparison between the two growth temperatures revealed only one temperature-induced change of the tRNA levels in the RNA-Seq data, which, however, did not overlap with another six found by MST. Correlation between MST and RNA-Seq showed only moderate R^2 values (Figure S7). Altogether, both datasets suggest that the tRNA levels in yeast are quite robust against temperature variation.

To further expand the scope of MST-based quantification, we established similar assays for other RNAs directly involved in translation. Thus FCPs developed against four rRNAs present in yeast ribosomes detected them in equal stochiometric amounts in isolated ribosomes (Figure S8). Furthermore, FCPs directed against polyadenylated RNA reflected differential poly-A length in synthetic mRNAs (Figure S9), recapitulated an increase in poly-A content in yeast cells after cycloheximide treatment, and detected differential poly-A content in HeLa versus HEK293 cells (Figure S10). However, and in contrast to the absolute tRNA quantification method developed above, these assays are only validated in relative terms.

In conclusion, we have developed a hybridization-based quantification method that is based on relatively simple considerations concerning titration experiments of a fixed concentration of an FCP with a dilution series of RNA preparations. Whereas EMSA allows the absolute quantification of a given RNA, MST yields quantitative data very fast and with outstanding precision. Strictly speaking, we have validated the accuracy of the method only for *E. coli* $tRNA^{Met}$. However, we have also obtained plausible data for various RNA species, for example, by reproducing literature data for the decay of yeast $tRNA^{Val}$ under RTD conditions,[12] by reproducing the correct stoichiometry of rRNA in ribosomes,[20] and by reproducing the known effect of CHX on polyA content of yeast RNA.[21] Beyond a basic characterization of the performance of MST-based quantification, our report contains new data with significant relevance for RNA biology, such as a direct comparison to RNA-Seq-based tRNA quantification, which clearly underscores the advantages of MST.

In summary, we posit that the unique combination of high precision with very short turnaround times makes MST-based quantification of nucleic acids a viable alternative to other hybridization-based techniques, and likely superior to RNA-Seq methods.

Acknowledgements

This work was supported by the DFG within the SPP1784 (HE3397/8-1, HE3397/13-2 to M.H.; SCHA750/20-2 to R.S.;

KL2937/1–2 to R.K.; RO4681/6-1 to J.-Y.R.: LE3260/2-1 to S.A.L.). Y.M. was supported by the ANR-DFG grant HTRNA-Mod ANR-13-ISV8-0001 and research funds from Lorraine Région (France). The collaboration was performed in the frame of the COST EPITRAN network. Support by the IMB Core Facility is acknowledged.

Conflict of interest

The authors declare no conflict of interest.

Keywords: fluorescence · hybridization · microscale thermophoresis · RNA quantification · tRNA stability

How to cite: *Angew. Chem. Int. Ed.* **2019**, *58*, 9565–9569
Angew. Chem. **2019**, *131*, 9666–9670

[1] a) H. Chang, J. Lim, M. Ha, V. N. Kim, *Mol. Cell* **2014**, *53*, 1044–1052; b) A. O. Subtelny, S. W. Eichhorn, G. R. Chen, H. Sive, D. P. Bartel, *Nature* **2014**, *508*, 66–71; c) J. Lim, M. Lee, A. Son, H. Chang, V. N. Kim, *Genes Dev.* **2016**, *30*, 1671–1682.

[2] a) A. E. Cozen, E. Quartley, A. D. Holmes, E. Hrabeta-Robinson, E. M. Phizicky, T. M. Lowe, *Nat. Methods* **2015**, *12*, 879–884; b) T. Gogakos, M. Brown, A. Garzia, C. Meyer, M. Hafner, T. Tuschl, *Cell Rep.* **2017**, *20*, 1463–1475; c) G. Zheng, Y. Qin, W. C. Clark, Q. Dai, C. Yi, C. He, A. M. Lambowitz, T. Pan, *Nat. Methods* **2015**, *12*, 835–837; d) Y. L. J. Pang, R. Abo, S. S. Levine, P. C. Dedon, *Nucleic Acids Res.* **2014**, *42*, e170.

[3] M. Jerabek-Willemsen, T. André, R. Wanner, H. M. Roth, S. Duhr, P. Baaske, D. Breitsprecher, *J. Mol. Struct.* **2014**, *1077*, 101–113.

[4] a) P. Baaske, C. J. Wienken, P. Reineck, S. Duhr, D. Braun, *Angew. Chem. Int. Ed.* **2010**, *49*, 2238–2241; *Angew. Chem.* **2010**, *122*, 2286–2290; b) S. A. I. Seidel et al., *Methods* **2013**, *59*, 301–315.

[5] F. Spenkuch, G. Hinze, S. Kellner, C. Kreutz, R. Micura, T. Basché, M. Helm, *Nucleic Acids Res.* **2014**, *42*, 12735–12745.

[6] M. Jerabek-Willemsen, C. J. Wienken, D. Braun, P. Baaske, S. Duhr, *Assay Drug Dev. Technol.* **2011**, *9*, 342–353.

[7] S. C. Wilson, D. T. Cohen, X. C. Wang, M. C. Hammond, *RNA* **2014**, *20*, 1153–1160.

[8] F. Juhling, M. Morl, R. K. Hartmann, M. Sprinzl, P. F. Stadler, J. Putz, *Nucleic Acids Res.* **2009**, *37*, D159–162.

[9] a) S. L. Hiley, J. Jackman, T. Babak, M. Trochesset, Q. D. Morris, E. Phizicky, T. R. Hughes, *Nucleic Acids Res.* **2005**, *33*, e2; b) Z. Paris, E. Horakova, M. A. Rubio, P. Sample, I. M. Fleming, S. Armocida, J. Lukes, J. D. Alfonzo, *RNA* **2013**, *19*, 649–658.

[10] S. Duhr, D. Braun, *Proc. Natl. Acad. Sci. USA* **2006**, *103*, 19678–19682.

[11] R. Klassen, J. P. Paluszynski, S. Wemhoff, A. Pfeiffer, J. Fricke, F. Meinhardt, *Mol. Microbiol.* **2008**, *69*, 681–697.

[12] A. Alexandrov, I. Chernyakov, W. Gu, S. L. Hiley, T. R. Hughes, E. J. Grayhack, E. M. Phizicky, *Mol. Cell* **2006**, *21*, 87–96.

[13] I. Chernyakov, J. M. Whipple, L. Kotelawala, E. J. Grayhack, E. M. Phizicky, *Genes Dev.* **2008**, *22*, 1369–1380.

[14] R. Klassen, A. Ciftci, J. Funk, A. Bruch, F. Butter, R. Schaffrath, *Nucleic Acids Res.* **2016**, *44*, 10946–10959.

[15] a) J. M. Whipple, E. A. Lane, I. Chernyakov, S. D'Silva, E. M. Phizicky, *Genes Dev.* **2011**, *25*, 1173–1184; b) S. Kadaba, A. Krueger, T. Trice, A. M. Krecic, A. G. Hinnebusch, J. Anderson, *Genes Dev.* **2004**, *18*, 1227–1240.

[16] Y. Motorin, M. Helm, *Biochemistry* **2010**, *49*, 4934–4944.

[17] R. Hauenschild et al., *Nucleic Acids Res.* **2015**, *43*, 9950–9964.

[18] a) F. Alings, L. P. Sarin, C. Fufezan, H. C. Drexler, S. A. Leidel, *RNA* **2015**, *21*, 202–212; b) L. Han, Y. Kon, E. M. Phizicky, *RNA* **2015**, *21*, 188–201; c) K. Tyagi, P. G. Pedrioli, *Nucleic Acids Res.* **2015**, *43*, 4701–4712; d) J. R. Damon, D. Pincus, H. L. Ploegh, *Mol. Biol. Cell* **2015**, *26*, 270–282.

[19] Q. Dai, G. Zheng, M. H. Schwartz, W. C. Clark, T. Pan, *Angew. Chem. Int. Ed.* **2017**, *56*, 5017–5020; *Angew. Chem.* **2017**, *129*, 5099–5102.

[20] M. Pospísek, L. Valásek, *Methods Enzymol.* **2013**, *530*, 173–181.

[21] V. Hilgers, D. Teixeira, R. Parker, *RNA* **2006**, *12*, 1835–1845.

Manuscript received: December 20, 2018
Accepted manuscript online: March 20, 2019
Version of record online: May 2, 2019

